

# **Intermolecular Interactions of Large Systems: Boron Nitrides, Acenes, and Coronenes**

Vladimir Fishman,<sup>†</sup> Jan M. L. Martin,<sup>†</sup> and A. Daniel Boese<sup>\*,‡</sup>

*†Department of Molecular Chemistry and Materials Science, Weizmann Institute of Science,  
7610001 Rehovot, Israel*

*‡Department of Chemistry, University of Graz, Heinrichstrasse 28/IV, 8010 Graz, Austria*

E-mail: adrian\_daniel.boese@uni-graz.at

## Abstract

In a recent contribution [Fishman, V.; Lesiuk, M.; Martin, J.M.L.; Boese, A.D. *J. Chem. Theory Comput.* **2025**, *21*, 2311–2324], we introduced another angle at benchmarking non-covalent interactions by not just benchmarking interaction energies of different species, but by considering the evolution of interaction energies with increasing system size.

Here, we extend the benchmark set to more species, such as electrostatically bound borazine dimers as well as the minima structures of parallel displaced acene and coronene dimers. While the minimum structures of the parallel displaced acene dimers yield similar results to previously published sandwich-structured acenes, the borazine dimers behave vastly different, yielding yet a more complete picture on non-covalent interactions and their scalability. In contrast, the polycyclic aromatic hydrocarbon structures – coronenes sandwich-stacked and coronenes parallel displaced – give results consistent with those obtained for both types of the polyacene series, resulting in an updated estimate for the coronene dimer energy.

## Introduction

Non-covalent interactions are at the forefront of modern science, as they determine the properties of many chemical systems, including molecular crystals,<sup>1</sup> solvents,<sup>2</sup> polymers,<sup>3,4</sup> proteins and nucleotides.<sup>5</sup> These interactions also control the self-assembly of nanomaterials,<sup>6</sup> drug docking processes,<sup>7</sup> liquids, and the binding of reaction partners in supramolecular catalysis.<sup>8</sup> Non-covalent interactions are weak contacts compared to covalent bonds and thus very sensitive to the environment. Therefore, their strength and nature should be predicted using robust, accurate quantum chemical methods with as few errors as possible.

In a *Nature Communications* paper from 2021,<sup>9</sup> a large discrepancy of 25% was found between two reference methods solving the Schrödinger equation differently, namely fixed-node diffusion Monte-Carlo (FN-DMC),<sup>10</sup> which is mainly used in solid state physics, and

coupled-cluster (CC) theory including singles, doubles, and perturbative triples CCSD(T)<sup>11,12</sup> — which has been termed the “gold standard” in gas phase quantum chemistry. The systems which showed these deviations were, however, too large to get some more insights by utilizing more elaborate methods than the ones used in the *Nature Communications* paper.

By considering the evolution of the correlation binding energy with respect to the number of subunits of dimer interactions,<sup>13</sup> we suggested to take another angle when benchmarking non-covalent interactions. Here, we do not look at mere energies, but deviations from the slopes of reference methods which scale linearly to ever larger systems. Specifically, we looked at the sandwich-stacked polyacene series as well as two geometries of alkapolyene dimers.

For the sandwich-stacked polyacene series, which is, as we will show later, closely related to the coronene dimer where some of the discrepancies between CCSD(T) and FN-DMC were found, we were able to perform CCSDT(Q)<sup>14</sup> calculations. Basically, CCSDT(Q) takes further terms in the coupled cluster approximation into account by including full triples and perturbative quadruples compared to CCSD(T), a method which has a much steeper scaling with system size, but is also rather close to the exact solution of the Schrödinger equation for closed-shell systems without much multi-reference character. By using this CCSDT(Q) estimate, we arrived<sup>13</sup> at a maximum deviation of 4.5% from CCSD(T) and not 25% for the buckycatcher, for which the largest discrepancy to FN-DMC was reported previously.<sup>9</sup> Furthermore, for the coronene *parallel displaced* dimer, we arrived at a maximum deviation of 3.5% between CCSDT(Q) and CCSD(T) and not 12% difference between CCSD(T) and FN-DMC. Summarizing, whereas CCSD(T) tended to overestimate the dissociation energies of pi-stacks, it did not at the large size suggested by FN-DMC. Similar results were also obtained for several polyaromatic hydrocarbon stacks including benzene using a simple underlying PPP Hamiltonian;<sup>15</sup> here, however, the CCSDT(Q) interaction energies exhibit larger dissociation energies than CCSD(T), which is in contrast to the results when a HF wavefunction is utilized.

Despite these results, all polyacenes and polyaromatic hydrocarbon stacks were investigated

before at their sandwich, i.e. transition state structures. One may argue that especially higher-order dispersion terms cancel at high symmetries, whereas at lower symmetries, they might not. For this purpose, we investigate parallel-displaced polyacene dimers which are global minimum structures for the polyacene series for naphthalene dimer and larger, and nearly isoenergetic<sup>16</sup> with the slanted T-shaped local minimum structure for the benzene dimer. Additionally, we explored sandwich-structured and parallel displaced coronene dimers. Furthermore, we considered two sandwich-like borazine dimer structures: One where the BN moiety is stacked towards NB, which exhibits a large electrostatic attraction, and the other one with the BN moiety stacked towards BN, yielding electrostatic repulsion.

This contribution is hence a direct continuation of our previous paper, introducing new species with (perfect) lines to interpolate. By using DFT-SAPT, we distinguish these species and devise them into different categories. Furthermore, we concentrate on aspects not investigated before, such as the non-linearity of different methods tested.

## Computational Details

We basically used the same methods and programs employed in our previous paper.<sup>13</sup> Calculations of the electronic structure have been performed using various software packages, depending on the method employed. Geometries of the investigated systems in the paper were optimized by density functional theory (DFT)<sup>17,18</sup> utilizing the  $\omega$ -B97M-V<sup>19</sup> functional with the def2-QZVPP<sup>20</sup> basis set using ORCA<sup>21</sup> 5.0.3. Full molecular symmetry was imposed.

To achieve highly accurate single-point energy calculations for the optimized investigated systems in our estimation and analysis, various forms of Coupled-Cluster (CC) theory were employed:

1. the “gold-standard” canonical CCSD(T) (Coupled-Cluster with Single, Double, and Perturbative Triple Excitations),<sup>11,12</sup> including its Resolution of Identity (RI), also called Density Fitting (DF),<sup>22,23</sup> for large systems, performed by the MRCC<sup>24</sup> program

package (August 2023 and later versions).

2. LNO (Local Natural Orbitals)-CCSD(T)<sup>25,26</sup> using the Normal, Tight, VeryTight and VeryVeryTight threshold settings with localcc=2021, performed by the same software.
3. DLPNO(Domain-Based Local Pair Natural Orbital)-CCSD(T<sub>1</sub>)<sup>27,28</sup> using the TightPNO threshold setting with two different values for the Pair Natural Orbital (PNO) truncation threshold (TCutPNO), specifically 10<sup>-6</sup> and 10<sup>-7</sup>, performed using ORCA<sup>21</sup> 5.0.4.
4. PNO(Pair Natural Orbital Local)-CCSD(T)<sup>29</sup> with DOMOPT Tight, DOMOPT vTight, and PAIROPT Tight truncation settings, performed by means of MOLPRO<sup>30</sup> 2024.3.
5. The CCSD(T) <sub>$\lambda$</sub>  method<sup>31-34</sup> — which treats the triples as a perturbation to CCSD — performed by CFOUR<sup>35</sup> program software. The CCSD(T) equations can be derived<sup>36</sup> by approximating the  $\Lambda$  vector as the transpose of the doubles amplitudes vector  $T_2$ .
6. Post-CCSD(T) methods, specifically CCSDT-2 and CCSDT-3,<sup>37</sup> for the first two species of each series investigated, were performed using CFOUR.<sup>35</sup>

For more approximate single-point energy calculations, we employed WFT (wavefunction theory)-based methods, including MP2(second-order Møller–Plesset perturbation theory)<sup>38</sup> using the MRCC<sup>24</sup> (August 2023) software and MP3 (third-order Møller–Plesset perturbation theory) with its RI implementation<sup>39</sup> in the Q-Chem<sup>40</sup> 6.1.0 program package. Additionally, we utilized DFT-based methods, specifically the dRPA (direct random-phase approximation) as implemented in MRCC<sup>24</sup> (August 2023) and DFT-SAPT(symmetry-adapted perturbation theory) as available in MOLPRO<sup>30</sup> 2022.2. These methods provided a lower-cost alternative for estimating correlation effects while maintaining a reasonable level of accuracy.

All single-point calculations were performed using the correlation-consistent<sup>41</sup> and augmented correlation-consistent<sup>42</sup> polarized valence X-zeta (X = D, T, Q, 5) basis sets for all systems. These will be abbreviated henceforth with DZ, TZ, QZ, 5Z, as well as aDZ, aTZ, aQZ, and a5Z, respectively.

# Results and Discussion

## Strong Correlation Diagnostics

To determine that our systems are well-described by single determinant methods, we evaluated a strong correlation diagnostic for all series based on total atomization energy (TAE) calculations obtained with the TZ basis set. The diagnostic methodology was taken from Ref. 43. The defining formulas are as follows:

$$\%TAE_X[\Delta X, \text{TPSS}] = 100\% \times \frac{(\text{TAE}[X, \text{TPSS@HF}] - \text{TAE}[X, \text{HF}])}{\text{TAE}[\text{CCSD(T)}]} \quad (1)$$

and

$$\%TAE_X[\Delta X, \text{KS} - \text{HF(TPSS)}] = 100\% \times \frac{(\text{TAE}[X, \text{TPSS@TPSS}] - \text{TAE}[X, \text{TPSS@HF}])}{\text{TAE}[\text{CCSD(T)}]} \quad (2)$$

The results show small static correlation around 5% for polyacene PD series and negligible static correlation, less than 2%, for borazines series , which, most importantly and interestingly, do not become larger when the number of rings increase.

## Different species investigated

In order to distinguish the different species that we investigated the slopes of, we explored the type of their intermolecular interactions by the use of symmetry-adapted perturbation theory (SAPT). We found both the induction  $E_{\text{ind}} = E_{\text{ind}}^{(2)} + E_{\text{ind-ex}}^{(2)} + E_{\Delta\text{HF}}$  to dispersion  $E_{\text{disp}} = E_{\text{disp}}^{(2)} + E_{\text{disp-ex}}^{(2)}$  and electrostatic  $E_{\text{elec}}^{(1)}$  to dispersion energy ratio<sup>44</sup> obtained from SAPT displayed in Table 1 as most instructive when trying to separate dispersion-dominated from induction-dominated systems. A more detailed analysis would analyse the percentage of the mean contribution of a fitted  $C_6$  term in the SAPT dispersion contribution, which is very small for induction-dominated systems.<sup>45</sup>

**Table 1: Different DFT-SAPT components (kJ/mol), induction to dispersion, and electrostatic to dispersion ratios using the cc-pV5Z basis set.**

Dimer	$E_{int}$	$E_{elec}^{(1)}$	$E_{ex}^{(1)}$	$E_{ind}$	$E_{disp}$	$\frac{E_{ind}}{E_{disp}}$	$\frac{E_{elec}^{(1)}}{E_{disp}}$
Benzene (sandwich)	-7.4	0.3	12.6	-0.8	-19.6	0.04	-0.02
Benzene (parallel displaced)	-11.8	-5.8	23.2	-2.6	-26.8	0.10	0.22
Ethylene	-0.4	1.1	1.0	-0.1	-2.4	0.04	-0.46
Borazine (syn)	-7.8	-2.0	15.2	-0.5	-20.5	0.02	0.10
Borazine (anti)	-13.0	-16.3	38.7	-2.2	-33.3	0.06	0.49
<hr/>							
Naphthalene (sandwich)	-17.1	-3.0	28.1	-1.3	-40.8	0.03	0.07
Naphthalene (parallel displaced)	-26.0	-15.5	50.6	-5.2	-56.0	0.09	0.28
Coronene (sandwich)	-57.8	-20.1	87.9	-1.9	-123.2	0.02	0.16
Coronene (parallel displaced)	-78.1	-36.6	114.1	-3.0	-145.3	0.02	0.25
Trans-Butadiene (relaxed)	-3.4	1.3	6.3	-0.5	-10.5	0.05	-0.12
Trans-Butadiene (fixed)	-2.5	1.8	1.7	-0.2	-5.7	0.04	-0.31
BN Naphthalene (syn)	-14.4	-4.3	29.5	-0.8	-38.9	0.02	0.11
BN Naphthalene (anti)	-25.3	-36.4	80.7	-4.8	-65.0	0.07	0.56

Based on the ratios reported in Table 1, four detached types of system can be distinguished. As noted in our previous paper, the  $\pi$ -stacks and alkapolyene stacks behave quite differently when compared to each other. This can be especially seen in the electrostatic to dispersion ratio, which is negative for the ethylene and trans-butadiene dimers, while it is positive for benzene and naphthalene (with the exception of sandwiched benzene, which is very slightly negative). As benzene and naphthalene have sizable quadrupole moments, this is visible in the electrostatic interaction between these species. The borazine and BN-naphthalene dimers are distinctly different again, as a partial charge can be found on the nitrogen (negative) and boron (positive) atoms. This is especially visible in the anti configuration, where we find the largest electrostatic contribution of all dimers. The syn configurations exhibit a more repulsive interaction which is, however, in its electrostatic component countered by the quadrupole and higher moments, making this configuration different again. We can already hypothesize that these species: alkapolyene stacks,  $\pi$ -stacks, borazine stacks (syn), and borazine stacks (anti) behave all quite differently, giving some insight about the nature of their intermolecular interaction.

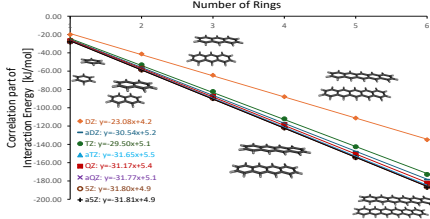
## Basis Set Effects

The starting point is to evaluate the basis set effects of the different methods. The correlation part of  $\pi$ -stacked molecules scales linearly with system size, yielding almost perfectly straight lines with  $R^2 > 0.99$  (Figure 1). Basis Set Effect LNO-CCSD(T) results with a Tight threshold are best suited, as calculations for 6-rings systems are feasible even in the a5Z basis set.

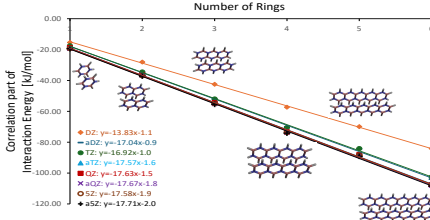
For the parallel displaced polyacene series counter-poise corrected slopes of aQZ, 5Z, a5Z basis sets are approximately the same quality as for the non-counterpoise (non-cp)-corrected slopes of the QZ, 5Z, a5Z basis sets. For the BN<sub>x</sub>\_NB<sub>x</sub> and BN<sub>x</sub>\_BN<sub>x</sub> series, we can observe a good match for aQZ and a5Z counterpoise (cp)-corrected slopes and for the 5Z and a5Z non-cp-corrected slopes.

Excluding the DZ basis set, the average cp-corrected slope is  $-31.18 \pm 1.68$  kJ/mol per ring for polyacene PD series,  $-17.44 \pm 0.53$  kJ/mol per ring for BN<sub>x</sub>\_NB<sub>x</sub> series, and  $-27.06 \pm 1.20$  kJ/mol per ring for BN<sub>x</sub>\_BN<sub>x</sub> series.

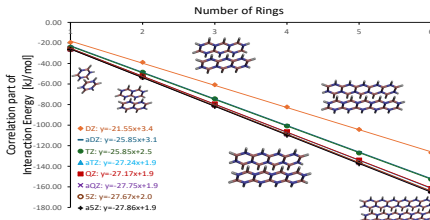
Intercepts, on the other hand, are much more sensitive to the basis set in all types of investigated systems, especially cp-uncorrected intercepts. Interestingly, the aDZ cp-uncorrected intercepts are even worse than the cp-uncorrected DZ ones (see subfigures d,e,f of Figure 1). Thus, for the aDZ basis set, there seems to be some imbalance introduced by the diffuse functions. Meanwhile, the aQZ intercepts reproduce the a5Z intercepts quite closely, which means that we can build an extrapolation over the aQZ results. Based on graphs Figure 1 a-c and corresponding cp-corrected slopes, we can summarize that the QZ basis set appears as the best compromise to get accurate slope values for a larger series of parallel displaced polyacenes and BN<sub>x</sub>\_BN<sub>x</sub>, while for BN<sub>x</sub>\_NB<sub>x</sub>, the aTZ basis set is even better. Practically, from a computational cost point of view, even the TZ basis set slopes will be satisfactory, because the deviation cp-corrected TZ slope from the cp-corrected a{Q,5}Z slope is only 5-8% (namely: 7% for polyacene PD dimers; 5% for BN<sub>x</sub>\_NB<sub>x</sub> and 8% for BN<sub>x</sub>\_BN<sub>x</sub>).



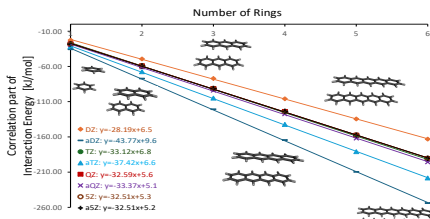
(a) cp-corrected energies for the acene series.



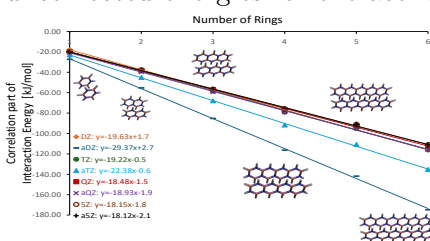
(b) cp-corrected energies for the BNx\_NBx series.



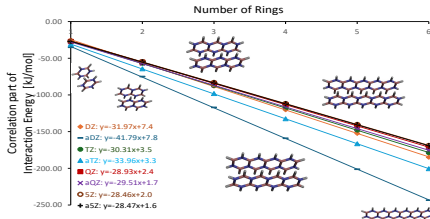
(c) cp-corrected energies for the BNx\_BNx series.



(d) cp-uncorrected energies for the acene series.



(e) cp-uncorrected energies for the BNx\_NBx series.



(f) cp-uncorrected energies for the BNx\_BNx series.

Figure 1: Correlation energies in kJ/mol vs. number of rings using the cc-pVnZ and aug-cc-pVnZ ( $n=D-5$ ) basis sets at the LNO-CCSD(T) level with Tight threshold including MP2 corrections.

## Local Correlation

Having established the basis set sensitivity, we turn to estimating canonical CCSD(T) results at the complete basis set limit. With the advent of local correlation methods in Coupled-Cluster theory and extrapolating their cutoff parameters, calculations of large systems become feasible and we can evaluate local methods to canonical CCSD(T) results. For this purpose, we compare results, obtained by several local coupled-cluster methods with the small DZ basis sets (both cp-corrected and cp-uncorrected DZ, see Figure 2), where we are capable to compare to canonical CCSD(T) for all systems. Again, perfect linear lines are observed for all variants of CCSD(T).

The first local variant investigated is local natural orbital (LNO) coupled-cluster, where the LNO cutoff threshold setting increases as Normal  $\rightarrow$  Tight  $\rightarrow$  very Tight  $\rightarrow$  very very Tight. Here, the slope converges toward to canonical CCSD(T) most of the times. When a cp-corrected DZ basis set is applied, the difference in slopes for polyacene PD systems when going from Normal to Tight to vTight to vvTight LNO thresholds to canonical CCSD(T) change by 2.73, 0.89, 0.14, 0.16 kJ/mol per subunit, showing a systematical convergence. For the BN<sub>x</sub>\_BN<sub>x</sub> series, no systematical convergence in the slope differences is observed, as the slopes change by: 2.28, 0.97, -0.10, -0.04 kJ/mol per subunit. Despite the fact that, as expected, LNO-CCSD(T)-vvTight gives the closest result to canonical-CCSD(T), the inequality is somewhat unexpectedly Normal  $\rightarrow$  Tight  $\rightarrow$  canonical  $\rightarrow$  vvTight  $\rightarrow$  vTight. For the BN<sub>x</sub>\_NB<sub>x</sub> series, the differences in slopes are 2.16, 0.63, -0.01, 0.10 kJ/mol per subunit, implying that the LNO-CCSD(T)-vTight slope value is closer to canonical-CCSD(T) than LNO-CCSD(T)-vvTight.

It should be pointed out that in our previous paper,<sup>13</sup> the last vTight point at the cp-corrected aTZ value was incorrect, resulting in an erroneous regression line in **Figure 2c** for LNO-CCSD(T)-vTight. The corresponding LNO-CCSD(T)-vTight line hence changes from  $y = -22.05 \cdot x - 1.6$  kJ/mol to  $y = -23.78 \cdot x + 2.4$  kJ/mol. The corrected **Figure 2c** for Ref. 13 is provided in the Supporting Information to the present paper.

Based on the foregoing analysis, LNO-CCSD(T) **underestimates** canonical-CCSD(T) in the calculation of non-covalent interaction energy for the polyacene PD and BN<sub>x</sub>\_NB<sub>x</sub> series. For the more electrostatically bound BN<sub>x</sub>\_BN<sub>x</sub> series, LNO **overestimates** canonical-CCSD(T).

Using the same DZ cp-corrected basis set for the second tested local method, Pair Natural Orbital Local CCSD(T) (PNO-LCCSD(T)), when going from the PAIROPT-TIGHT threshold to DOMOPT-TIGHT to DOMOPT-VTIGHT to canonical CCSD(T), the slopes change by -0.70, -0.34, -0.73 kJ/mol per subunit for the polyacene PD series, respectively. Thus, PNO-LCCSD(T) is showing a systematical convergence, but with negative sign, unlike the LNO approximation. For the PNO approximation, a similar trend of convergence is observed for the BN<sub>x</sub>\_NB<sub>x</sub> series, where the slopes change by -0.29, -0.41, -0.01 kJ/mol per subunit. In contrast, for the BN<sub>x</sub>\_BN<sub>x</sub> series, a non-systematical convergence of slopes is observed, changing by -1.09, -0.56, +0.11 kJ/mol per subunit. For all types of local methods applied, the PNO-LCCSD(T) approximation gives the closest slope to canonical CCSD(T) with the DOMOPT-VTIGHT parameter.

As a third method, domain-based Local Pair Natural Orbital Coupled-Cluster (DLPNO-CCSD(T<sub>1</sub>)) was utilized. Here — even when employing counterpoise corrections — we cannot make a definitive conclusion regarding the optimal TCut parameter for the DLPNO approximation. For the polyacene PD series, the TCut=1e-6 cutoff yields a slope closer in value to canonical CCSD(T). For the BN<sub>x</sub>\_BN<sub>x</sub> series, TCut=1e-7 yields closer result, while for BN<sub>x</sub>\_NB<sub>x</sub> series both cutoff parameters are equally far from the canonical CCSD(T) slope.

As discussed in the previous section, the deviation of counterpoise (cp)-corrected TZ slopes is imperceptible from a{Q,5}Z. Hence, the analysis of results obtained with the TZ basis is possibly better, although we have less species to compare to. As far as canonical-CCSD(T)/TZ calculations are doable for at least four systems in each series, we can consider the convergence for different local coupled-cluster theories to canonical-CCSD(T) for the 1→4

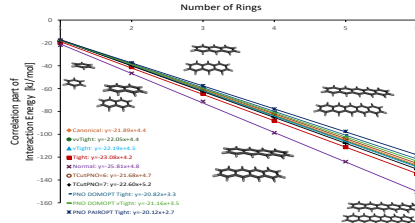
TZ Slope. The convergence for PNO-LCCSD(T) approximation has the trend PAIROPT-TIGHT → DOMOPT-TIGHT → DOMOPT-VTIGHT → canonical for all systems.

For LNO-CCSD(T) in combination with the cp-corrected TZ basis set, the thresholds converge as expected with increasing cutoffs: `Normal` → `Tight` → `VeryTight` → `VeryVeryTight` → canonical. The same is happening for the cp-uncorrected TZ basis set with the exception of the BN<sub>x</sub>\_BN<sub>x</sub> series, in which, interestingly, the `Tight` threshold reproduces the canonical result with the lowest deviation.

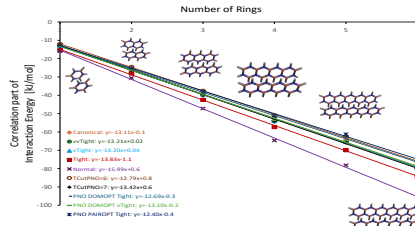
For the DLPNO approximation, the BN<sub>x</sub>\_NB<sub>x</sub> series is not as convergent for the different cut-offs in case of cp-corrected TZ basis set: The `TCut=1e-6` parameter overestimates canonical results, while `TCut=1e-7` underestimates it. The discrepancy of `TCut=1e-6` is twice as large as for `TCut=1e-7`. In all other cases, each series converges from `TCut=1e-6` → `TCut=1e-7` → canonical.

## Electronic Structure Methods

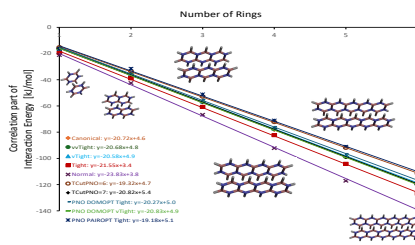
Having estimated the slopes of canonical basis set limit CCSD(T) and thus its performance for large molecules, we evaluate the efficiency of more approximate electronic structure methods. Here, we investigate several post-Hartree-Fock methods, such as MP2, MP2.5, MP3; the dispersion contribution of DFT-SAPT, as well as dRPA. To determine the degree of agreement of the approximate methods with the “gold standard” canonical CCSD(T), we compared absolute values of slopes obtained using these approximate methods. For the parallel displaced polyacene systems the trend MP3 < CCSD < dRPA ≈ CCSD(T) ≈ DFT-SAPT < MP2.5 < MP2 is observed for cp-corrected and cp-uncorrected (excluding DFT-SAPT for the latter, as DFT-SAPT is only defined when using cp-corrections) slope values. As was described earlier for sandwich polyacene dimers (see section ”Electronic Structure Methods” in Ref. 13), for the parallel displaced polyacene dimers, MP2 also significantly overestimates interaction energies whereas MP3 significantly underestimates them and, which is as well important to note, DFT-SAPT and dRPA are closer to CCSD(T) than the post-Hartree-Fock methods



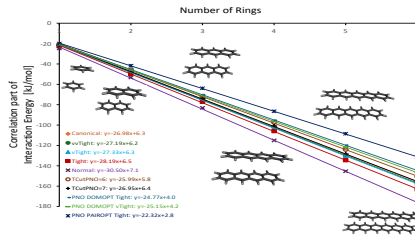
(a) cp-corrected DZ energies for the acene PD series.



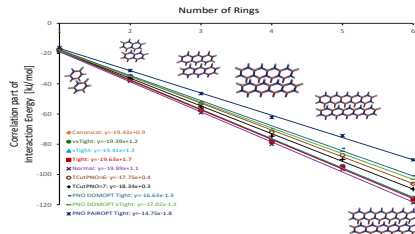
(b) cp-corrected DZ energies for the BN<sub>x</sub>\_NB<sub>x</sub> series.



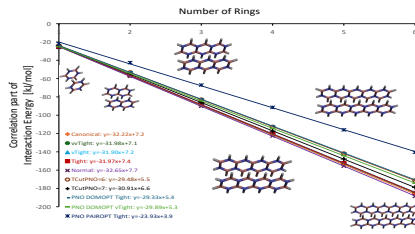
(c) cp-corrected DZ energies for the BN<sub>x</sub>-BN<sub>x</sub> series.



(d) cp-uncorrected DZ energies for the acene PD series.



(e) cp-uncorrected DZ energies for the BN<sub>x</sub> NB<sub>x</sub> series.



(f) cp-uncorrected DZ energies for the BN<sub>x</sub>-BN<sub>x</sub> series.

Figure 2: Correlation energies (kJ/mol) derived from various coupled cluster methods in as a function of system size per number of rings. 13

investigated.

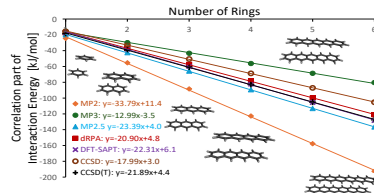
An identical trend for cp-corrected slope values is observed for BN<sub>x</sub>-NB<sub>x</sub> dimers. Here, deviations of MP2 and MP3 slopes are not as large from CCSD(T) (12% and 23% respectively), while for polyacene dimers the same deviations is as big as 50%. In this case, dRPA demonstrates the best approximation to CCSD(T).

In case of cp-uncorrected slope values for the BN<sub>x</sub>-NB<sub>x</sub> dimers, the MP2 and MP2.5 methods are the best approximation to CCSD(T), while MP3 still underestimates interaction energies. This is in contrast to the polyacene PD, where the slope of the BN<sub>x</sub>-BN<sub>x</sub> systems exhibit a very different behavior: MP3 < CCSD < MP2.5 < CCSD(T) < MP2 < dRPA < DFT-SAPT. Here, DFT-SAPT and dRPA are, interestingly, inferior to the MP2.5 and MP2 methods, whereas MP3 still noticeably underestimates interaction energies.

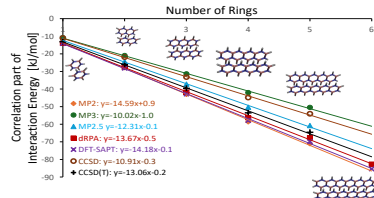
## Best Estimates of Slopes

As long as many calculations using the “gold-standard” canonical CCSD(T) method are doable only with the DZ basis set, we can either calculate each system which belongs to the investigated sequence with this rather poor basis set, or increase the basis set size and calculate less number of systems, thus adding an additional dimension to the problem. Unfortunately, CCSDT and CCSDT(Q) calculations for the naphthalene parallel-displaced or borazine sandwich dimers are currently computationally not feasible even with a “truncated” DZ basis set with no *p*-functions on Hydrogen. Instead, we consider CCSDT-2 and CCSDT-3<sup>37</sup> instead of CCSDT, as they scale as  $O(N^7)$  rather than the  $O(N^8)$  with the number of electrons. Also, we can estimate the CCSDT(Q) deviations of CCSD(T) with CCSD(T) <sub>$\lambda$</sub> , as the correlation part of CCSD(T) <sub>$\lambda$</sub>  seems to be somewhat closer to the correlation part of CCSDT(Q) than CCSD(T) (See Figure 4, SI of Ref. 13 and Ref. 46).

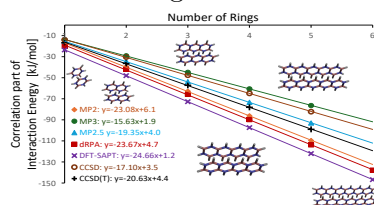
Here, the polyacene parallelly displaced series is rather important, since we can compare the behavior of their slopes with the previous polyacene sandwich-structure results. BN<sub>x</sub>-NB<sub>x</sub> and BN<sub>x</sub>-BN<sub>x</sub> do not support extended uniform  $\pi$ -delocalization and their aromaticity is



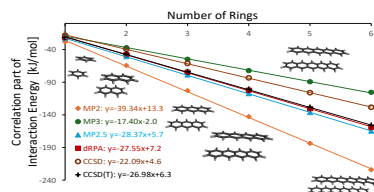
(a) cp-corrected DZ energies for the acene PD series.



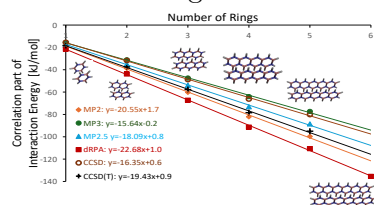
(b) cp-corrected DZ energies for the BNx\_NBx series.



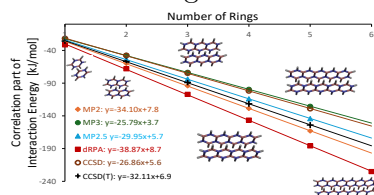
(c) cp-corrected DZ energies for the BNx\_BNx series.



(d) cp-uncorrected DZ energies for the acene PD series.



(e) cp-uncorrected DZ energies for the BNx\_NBx series.



(f) cp-uncorrected DZ energies for the BNx\_BNx series.

Figure 3: Correlation energies derived from various post-Hartree-Fock (and DFT) methods in kJ/mol vs. number of rings.

reduced, polarized, and not sextet based. Meanwhile, the polyacenes have a delocalized and non-polar pi-electron distribution and their electronic structure is more predictable by carbon topology, as all electronic structure methods behave rather similar to the polyacenes.

The slopes of the correlation energy, extrapolated to cp-uncorrected and cp-corrected complete basis set limits, for all investigated series are summarized in Table 2, while Table 3 summarizes the slopes of the full interaction energies obtained by different WFT-based methods.

**Table 2: Best available Correlation Energy Slopes (kJ/mol per Subunit)<sup>a</sup>**

System	Method									
	CCSD(T)					post-CCSD(T)				
	MP2	CCSD	Tight	VeryTight	canonical	CCSD(T) <sub>λ</sub>	CCSDT-2	CCSDT-3	CCSDT	CCSDT(Q)
BN <sub>x</sub> _NB <sub>x</sub>	-19.58	-14.16	-17.75	-17.59	-17.52	-17.44 <sup>b</sup>	-17.15 <sup>b</sup>	-17.28 <sup>b</sup>		
BN <sub>x</sub> _BN <sub>x</sub>	-30.97	-22.79	-27.98	-27.96	-28.24	-28.00 <sup>b</sup>	-27.49 <sup>b</sup>	-27.69 <sup>b</sup>		
Acene PD	-45.15	-24.55	-31.85	-31.37	-31.04	-30.74 <sup>b</sup>	-30.24 <sup>b</sup>	-30.30 <sup>b</sup>		
Acenes <sup>c</sup>	-33.91	-18.33	-24.62	-24.13	-23.20	-22.98 <sup>b</sup>	-22.51 <sup>b</sup>	-22.55 <sup>b</sup>	-22.16 <sup>b</sup>	-22.72 <sup>b</sup>
Polyene Relax.	-11.02	-7.06			-8.75	-8.64 <sup>b</sup>	-8.55 <sup>b</sup>	-8.57 <sup>b</sup>	-8.55 <sup>b</sup>	-8.78 <sup>b</sup>
Polyene Fixed	-4.87	-3.06			-3.82	-3.78 <sup>b</sup>	-3.73 <sup>b</sup>	-3.74 <sup>b</sup>	-3.72 <sup>b</sup>	-3.82 <sup>b</sup>
Coronene PD	-31.51	-16.37	-21.72	-20.93	-20.43	-20.24 <sup>b</sup>			-19.67 <sup>d</sup>	-20.18 <sup>d</sup>
Coronene Sandwich	-28.08	-14.91	-20.15	-19.41	-18.72	-18.58 <sup>b</sup>				
BN <sub>x</sub> _NB <sub>x</sub>	-19.20	-13.87	-17.27	-16.88	-17.15	-17.02 <sup>b</sup>	-16.71 <sup>b</sup>	-16.85 <sup>b</sup>		
BN <sub>x</sub> _BN <sub>x</sub>	-30.41	-22.25	-27.38	-27.36	-27.65	-27.34 <sup>b</sup>	-26.74 <sup>b</sup>	-26.94 <sup>b</sup>		
Acene PD	-44.63	-24.02	-31.61	-30.93	-30.50	-30.04 <sup>b</sup>	-29.39 <sup>b</sup>	-29.46 <sup>b</sup>		
Acenes <sup>c</sup>	-34.20	-18.32	-24.31	-23.90	-23.18	-22.91 <sup>b</sup>	-22.40 <sup>b</sup>	-22.45 <sup>b</sup>	-22.08 <sup>b</sup>	-22.64 <sup>b</sup>
Polyene Relax.	-11.04	-7.00			-8.68	-8.57 <sup>b</sup>	-8.46 <sup>b</sup>	-8.49 <sup>b</sup>	-8.45 <sup>b</sup>	-8.69 <sup>b</sup>
Polyene Fixed	-4.86	-3.01			-3.83	-3.88 <sup>b</sup>	-3.83 <sup>b</sup>	-3.84 <sup>b</sup>	-3.76 <sup>b</sup>	-3.94 <sup>b</sup>
Coronene PD	-31.04	-16.07	-21.47	-20.77	-20.19	-19.92 <sup>b</sup>				
Coronene Sandwich	-27.26	-14.37	-19.64	-18.89	-18.08	-17.90 <sup>b</sup>				

<sup>a</sup> Numbers in italics are estimates. All slopes given for the aug-cc-pVQ{Q,5}Z basis set. The top part of the Table shows the cp-corrected results, the bottom part the cp-uncorrected ones. Detailed Tables are given in the SI.

<sup>b</sup> The post-CCSD(T) slopes have been scaled by a factor of 1.4 to account for the small cc-pVDZ basis set size — see discussion in<sup>13</sup> and in its Supporting Information.

<sup>c</sup> Re-estimated values for sandwich-structured acene series with the most recent MRCC version.

<sup>d</sup> CCSDT and CCSDT(Q) slopes for Coronene PD have been estimated according to respective difference with CCSD(T) for hexacene sandwich-structured dimer - see discussion below.

The CCSD(T) 1 → 6 CBS lines for all our systems are obtained as follows:

$$y = (-6.7 \pm 0.2 \text{ kJ/mol}) \cdot x + -0.5 \pm 0.1 \text{ kJ/mol}$$

per ring including HF for BN<sub>x</sub>\_NB<sub>x</sub> series,

$$y = (-17.1 \pm 0.1 \text{ kJ/mol}) \cdot x + 4.8 \pm 1.2 \text{ kJ/mol}$$

per ring including HF for BN<sub>x</sub>-BN<sub>x</sub> series, and

$$y = (-16.2 \pm 0.3 \text{ kJ/mol}) \cdot x + 6.3 \pm 0.1 \text{ kJ/mol}$$

per ring including HF for the parallel displaced polyacene series. The best estimate CCSD(T)<sub>λ</sub> interaction energies for the benzene and naphthalene parallel displaced dimers are  $-10.8 \pm 0.2$  and  $-25.2 \pm 0.9 \text{ kJ/mol}$  respectively, resulting in a slope value of  $-14.4 \text{ kJ/mol}$  per subunit, similar to the one discussed above.

**Table 3: Best available aug-cc-pV{Q,5}Z Energy Slopes, including Hartree-Fock (kJ/mol per Subunit)<sup>a</sup> with reference to Table 2**

System	MP2	CCSD	CCSD(T)				post-CCSD(T)			
			Tight	VeryTight	canonical	CCSD(T) <sub>λ</sub>	CCSDT-2	CCSDT-3	CCSDT	CCSDT(Q)
BN <sub>x</sub> -NB <sub>x</sub>	<i>-9.03</i>	<i>-3.61</i>	-7.19	-7.03	-6.96	-6.88 <sup>b</sup>	-6.60 <sup>b</sup>	-6.73 <sup>b</sup>		
BN <sub>x</sub> -BN <sub>x</sub>	<i>-20.01</i>	<i>-11.83</i>	-17.02	-17.00	-17.27	-17.04 <sup>b</sup>	-16.52 <sup>b</sup>	-16.73 <sup>b</sup>		
Acene PD	<i>-30.68</i>	<i>-10.09</i>	-17.39	-16.91	-16.58	-16.28 <sup>b</sup>	-15.78 <sup>b</sup>	-15.84 <sup>b</sup>		
Acenes <sup>c</sup>	<i>-21.95</i>	<i>-6.38</i>	-12.66	-12.17	-11.24	-11.02 <sup>b</sup>	-10.55 <sup>b</sup>	-10.59 <sup>b</sup>	-10.20 <sup>b</sup>	-10.76 <sup>b</sup>
Polyene Relax.	<i>-5.70</i>	<i>-1.74</i>			-3.43	-3.32 <sup>b</sup>	-3.23 <sup>b</sup>	-3.25 <sup>b</sup>	-3.23 <sup>b</sup>	-3.45 <sup>b</sup>
Polyene Fixed	<i>-3.36</i>	<i>-1.54</i>			-2.31	-2.27 <sup>b</sup>	-2.22 <sup>b</sup>	-2.23 <sup>b</sup>	-2.21 <sup>b</sup>	-2.31 <sup>b</sup>
Coronene PD	<i>-23.06</i>	<i>-7.93</i>	-13.28	-12.49	-11.98	-11.79 <sup>b</sup>			-11.23 <sup>d</sup>	-11.74 <sup>d</sup>
Coronene Sandwich	<i>-18.42</i>	<i>-5.25</i>	-10.49	-9.75	-9.06	-8.92 <sup>b</sup>				
BN <sub>x</sub> -NB <sub>x</sub>	<i>-8.54</i>	<i>-3.21</i>	-6.62	-6.22	-6.49	-6.36 <sup>b</sup>	-6.05 <sup>b</sup>	-6.19 <sup>b</sup>		
BN <sub>x</sub> -BN <sub>x</sub>	<i>-19.78</i>	<i>-11.62</i>	-16.74	-16.73	-17.01	-16.70 <sup>b</sup>	-16.11 <sup>b</sup>	-16.31 <sup>b</sup>		
Acene PD	<i>-30.03</i>	<i>-9.41</i>	-17.00	-16.32	-15.90	-15.44 <sup>b</sup>	-14.78 <sup>b</sup>	-14.86 <sup>b</sup>		
Acenes <sup>c</sup>	<i>-22.33</i>	<i>-6.46</i>	-12.45	-12.04	-11.31	-11.04 <sup>b</sup>	-10.54 <sup>b</sup>	-10.58 <sup>b</sup>	-10.21 <sup>b</sup>	-10.77 <sup>b</sup>
Polyene Relax.	<i>-5.65</i>	<i>-1.61</i>			-3.29	-3.18 <sup>b</sup>	-3.07 <sup>b</sup>	-3.10 <sup>b</sup>	-3.06 <sup>b</sup>	-3.30 <sup>b</sup>
Polyene Fixed	<i>-3.30</i>	<i>-1.46</i>			-2.27	-2.33 <sup>b</sup>	-2.27 <sup>b</sup>	-2.29 <sup>b</sup>	-2.21 <sup>b</sup>	-2.38 <sup>b</sup>
Coronene PD	<i>-22.49</i>	<i>-7.52</i>	-12.92	-12.22	-11.64	-11.37 <sup>b</sup>				
Coronene Sandwich	<i>-17.50</i>	<i>-4.62</i>	-9.89	-9.13	-8.33	-8.14 <sup>b</sup>				

<sup>a</sup> Numbers in italics are estimates. All slopes given for the aug-cc-pV{Q,5}Z basis set. The top part of the Table shows the cp-corrected results, the bottom part the cp-uncorrected ones.

<sup>b</sup> The post-CCSD(T) slopes have been scaled by a factor of 1.4 to account for the small cc-pVDZ basis set size — see discussion in<sup>13</sup> and in its Supporting Information.

<sup>c</sup> Re-estimated values for sandwich-structured acene series with the most recent MRCC version.

<sup>d</sup> CCSDT and CCSDT(Q) slopes for Coronene PD have been estimated according to respective difference with CCSD(T) for hexacene sandwich-structured dimer.

## Coronene Dimer

Of special interest is the radially fused and parallel displaced polycyclic aromatic hydrocarbon series going from Benzene  $\rightarrow$  Coronene  $\rightarrow$  Circumcoronene.

Following the same recipe of Slope and Intercept estimation as above (see also SI), we are able to estimate the interaction energy of the parallel displaced coronene dimer. Table 4 shows the interaction energy of the parallel displaced coronene dimer at different levels of computational theory with various estimation techniques. Here, our CCSD(T)/CBS result fits well with the tendency that the LNO approximation systematically **underestimates** canonical CCSD(T) correlation energy (as shown in Figure 2), i.e. **overestimates** the **absolute** canonical interaction energy for hydrocarbon systems.

During the re-evaluation of the interaction energies for sandwich-structured polyacene series, we noticed that the  $[(T)_\lambda - (T)]/\text{CBS(cp-corr)}$  difference for sandwich-structured hexacene dimer, which is 1.34 kJ/mol, is surprisingly close to the  $[(T)_\lambda - (T)]/\text{CBS(cp-corr)}$  difference for the parallel displaced coronene dimer of 1.37 kJ/mol. Assuming a similar behavior of other post-CCSD(T) corrections for  $\pi$ -conjugated aromatic systems, we estimate the  $(Q) - (T)$  difference for coronene PD to be expressed mathematically through a  $(Q) - (T)$  difference for sandwich-structured hexacene, such as:

$$[(Q) - (T)]_{\text{coronene PD}} \approx [(T)_\lambda - (T)]_{\text{coronene PD}} \times [(Q) - (T)]_{\text{hexacene}} \div [(T)_\lambda - (T)]_{\text{hexacene}} \quad (3)$$

This is resulting in an estimate of  $[(Q) - (T)]_{\text{coronene PD}} \approx 1.37 \times 2.87 \div 1.34 = 2.95 \text{ kJ/mol}$ . Thus, the CCSDT(Q)/CBS(cp-corr) interaction energy for the parallel displaced coronene dimer is estimated as -80.3 kJ/mol. The same estimation for the  $T_3 - (T)$  contribution yields an interaction energy of -76.7 kJ/mol at the CCSDT/CBS level.

Additionally, we can estimate the interaction energy for the even larger sandwich-stacked circumcoronene ( $C_{54}H_{18}$ ) dimer, where each monomer contains 19 benzene rings.

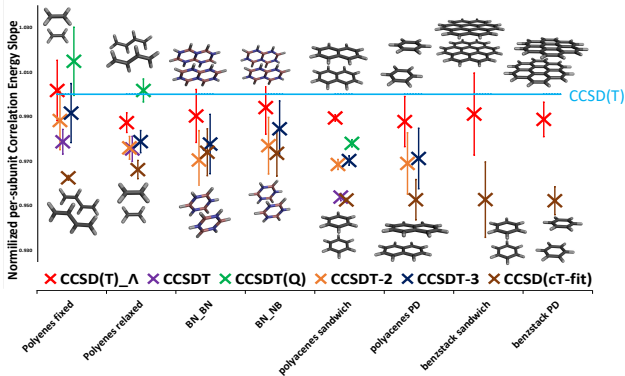


Figure 4: Deviations of Correlation energies from reference CCSD(T) method in kJ/mol vs. number of subunits.

**Table 4: Interaction energies for the coronene PD dimer at the different level of theory in complete basis set. All values are reported in kJ/mol.**

Level of Theory	Interaction energy	Reference
MP2	$-161.1 \pm 2.1$	Table 1 in Ref. 47
MP2	-159.3	Table S1 in Ref. 48
MP2	-157.9 (cp-corr)	this work
CCSD	$-56.1 \pm 2.1$	Table 1 in Ref. 47
CCSD	-54.0 (cp-corr)	this work
DLPNO-CCSD( $T_0$ )	$-87.6 \pm 1.8$	Table 1 in Ref. 48
PNO-LCCSD(T)-F12 (domopt=tight)	-83.6 (cp-corr)	Table 10 in Ref. 29
PNO-LCCSD(T)-F12-Tight+	-80.8 (cp-corr)	Table 6 in Ref. 49
PNO-LCCSD( $T^*$ )-F12-Tight+	-83.7 (cp-corr)	Table 6 in Ref. 49
LNO-CCSD(T)	$-86.2 \pm 2.5$	Table 1 in Ref. 9
LNO-CCSD(T)-vTight	$-85.2 \pm 1.2$	this work
CCSD(T)	-86.4	Table 4,5 in Ref. 50
CCSD(T)	$-88.3 \pm 2.1$	Table 1 in Ref. 47
CCSD(cT)	$-80.8 \pm 2.1$	Table 1 in Ref. 47
CCSD(T)	-83.2 (cp-corr)	this work
CCSD(T) $_{\lambda}$	-81.9 (cp-corr)	this work
CCSDT(Q)*	-80.3 (cp-corr)	this work
FN-DMC	$-75.7 \pm 3.3$	Table 1 in Ref. 9
FN-DMC	$-73.2 \pm 2.9$	Table 1 in Ref. 51
CCSDT*	-76.7 (cp-corr)	this work

\* CCSDT and CCSDT(Q) cp-corrected results have been estimated according to respective difference with CCSD(T) for hexacene sandwich-structured dimer.

The CCSD(T) slope and intercept for the sandwich-structured radially fused polycyclic aromatic hydrocarbons is

$$y = -9.06 \cdot x + 1.82 \text{ kJ/mol}$$

per ring for cp-corrected interaction energy, resulting in an interaction energy of -170.4 kJ/mol for the circumcoronene dimer.

If we extrapolate only the CCSD(T) correlation energy and then add the Hartree-Fock energy, we obtain  $-18.72 \cdot 19 - 3.18 + 164.52 = -194.4$  kJ/mol as cp-corrected result. Meanwhile, the LNO-CCSD(T)-Tight correlation energy aligns well with a linear trend (see SI), yielding a coefficient of determination  $R^2 > 0.999$ . Our best estimate cp-corr CCSD(T) $_{\lambda}$  interaction energy for the sandwich-stacked circumcoronene–coronene dimer is thus -191.6 kJ/mol which is close to the cp-corr CCSD(T)/CBS result.

Finally, it appears that a non-negligible part (of 3.0 kJ/mol) of the discrepancy between CCSD(T) and DMC of reference 9 can be attributed to the overestimation of canonical CCSD(T) with local methods, the second part (2.9 kJ/mol- in reference 13, we estimated this value to a maximum of 3.2 kJ/mol) then comes from higher-order cluster excitations when going from CCSD(T) to CCSDT(Q), and the rest (4.6 kJ/mol) from FN-DMC probably underestimating the result because of the fixed-node approximation.<sup>52–55</sup> This is implying that the true result is pretty much in between canonical, corrected CCSD(T) and FN-DMC, but slightly closer to CCSD(T).

## Conclusions

Extending upon the correlation energy slopes of the alkapolyene (fixed and relaxed geometries) and sandwich polyacene series, we investigated five more series looking at non-covalent interactions. The new series include the minimum, parallel displaced polyacene structures, as well as the two BN analogues of the sandwich polyacenes and both parallel displaced and sandwich coronene series structures. With these, we are capable to draw a more complete

picture of the nature of non-covalent interactions beyond small model systems, as their performance when going to larger sizes is explored. All the computed series are exhibiting a near-linear behavior.

By considering local correlation thresholds, basis sets, and different methods, we can draw conclusions on their scaling behavior. For local orbital approximations of the coupled-cluster method, only the tightest threshold settings (vvTight for LNO-CCSD(T) and DO-MOPT=vTight for PNO-LCCSD(T)) achieve near-canonical-CCSD(T) accuracy. Overall, the basis set limit for the slopes is much quicker accomplished than for the intercepts, making calculations of slopes computationally less demanding.

In general, the polyacene and coronene systems behave quite similar, even if for the latter, the system size grows explosively like the number of rings in radially fused polycyclic aromatic hydrocarbons, *viz.*  $1 \rightarrow 7 \rightarrow 19 \rightarrow 37$ .

Finally, we are able to show that for the parallel displaced coronene dimer the higher-order triples are antibonding, which bring CCSDT interaction energies closer to DMC, whereas CCSDT(Q) tends to get back closer to the CCSD(T) method, with the final value being slightly closer to the CCSD(T) than the DMC value, reconfirming our previous results.

## Acknowledgments

This research was supported by an internal grant to JMLM from the Uriel Arnon Memorial Fund for Artificial Intelligence in Materials Research. All calculations were carried out on the Faculty of Chemistry's high-performance computing facility CHEMFARM, which is supported in part by the Ben May Center for Chemical Theory and Computation. The authors thank its administrators, Dr. Mark Vilensy and Andrei Vasilev, for their kind assistance.

ADB was supported by the Weizmann Institute of Science as a Weston Visiting Scholar.

## Supporting Information Available

- PDF document with full raw data, including additional discussions, extra methods used, data for further polyaromatic systems, can be found in the Supporting Information.
- Cartesian coordinate (xyz) files of the structures used in this paper are given.

## References

- (1) Saleh, G.; Gatti, C.; Lo Presti, L.; Contreras-García, J. Revealing non-covalent interactions in molecular crystals through their experimental electron densities. *Chem. Eur. J.* **2012**, *18*, 15523–15536, DOI: [10.1002/chem.201201290](https://doi.org/10.1002/chem.201201290).
- (2) Storer, M. C.; Hunter, C. A. The surface site interaction point approach to non-covalent interactions. *Chem. Soc. Rev.* **2022**, *51*, 10064–10082, DOI: [10.1039/D2CS00701K](https://doi.org/10.1039/D2CS00701K).
- (3) Buaksuntar, K.; Limarun, P.; Suethao, S.; Smithipong, W. Non-covalent interaction on the self-healing of mechanical properties in supramolecular polymers. *International Journal of Molecular Sciences* **2022**, *23*, 6902, DOI: [10.3390/ijms23136902](https://doi.org/10.3390/ijms23136902).
- (4) Chen, J.; Peng, Q.; Peng, X.; Zhang, H.; Zeng, H. Probing and manipulating noncovalent interactions in functional polymeric systems. *Chem. Rev.* **2022**, *122*, 14594–14678, DOI: [10.1021/acs.chemrev.2c00215](https://doi.org/10.1021/acs.chemrev.2c00215).
- (5) Adhav, V. A.; Saikrishnan, K. The realm of unconventional noncovalent interactions in proteins: their significance in structure and function. *ACS Omega* **2023**, *8*, 22268–22284, DOI: [10.1021/acsomega.3c00205](https://doi.org/10.1021/acsomega.3c00205).
- (6) Tuncel, D. Non-covalent interactions between carbon nanotubes and conjugated polymers. *Nanoscale* **2011**, *3*, 3545–3554, DOI: [10.1039/C1NR10338E](https://doi.org/10.1039/C1NR10338E).

(7) Rehman, S. U.; Sarwar, T.; Husain, M. A.; Ishqi, H. M.; Tabish, M. Studying non-covalent drug–DNA interactions. *Archives of Biochemistry and Biophysics* **2015**, *576*, 49–60, DOI: [10.1016/j.abb.2015.04.004](https://doi.org/10.1016/j.abb.2015.04.004).

(8) Raynal, M.; Ballester, P.; Vidal-Ferran, A.; van Leeuwen, P. W. Supramolecular catalysis. Part 1: non-covalent interactions as a tool for building and modifying homogeneous catalysts. *Chem. Soc. Rev.* **2014**, *43*, 1660–1733, DOI: [10.1039/C3CS60027K](https://doi.org/10.1039/C3CS60027K).

(9) Al-Hamdani, Y. S.; Nagy, P. R.; Zen, A.; Barton, D.; Kállay, M.; Brandenburg, J. G.; Tkatchenko, A. Interactions between large molecules pose a puzzle for reference quantum mechanical methods. *Nat. Commun.* **2021**, *12*, 3927, DOI: [10.1038/s41467-021-24119-3](https://doi.org/10.1038/s41467-021-24119-3).

(10) Reynolds, P. J.; Ceperley, D. M.; Alder, B. J.; Lester Jr, W. A. Fixed-node quantum Monte Carlo for molecules. *J. Chem. Phys.* **1982**, *77*, 5593–5603, DOI: [10.1063/1.443766](https://doi.org/10.1063/1.443766).

(11) Raghavachari, K.; Trucks, G. W.; Pople, J. A.; Head-Gordon, M. A Fifth-Order Perturbation Comparison of Electron Correlation Theories. *Chem. Phys. Lett.* **1989**, *157*, 479–483, DOI: [10.1016/S0009-2614\(89\)87395-6](https://doi.org/10.1016/S0009-2614(89)87395-6).

(12) Gyevi-Nagy, L.; Kállay, M.; Nagy, P. R. Integral-direct and parallel implementation of the CCSD(T) method: Algorithmic developments and large-scale applications. *J. Chem. Theory Comput.* **2020**, *16*, 366, DOI: [10.1021/acs.jctc.9b00957](https://doi.org/10.1021/acs.jctc.9b00957).

(13) Fishman, V.; Lesiuk, M.; Martin, J. M.; Boese, A. D. Another angle on benchmarking noncovalent interactions. *J. Chem. Theory Comput.* **2025**, *21*, 2311–2324, DOI: [10.1021/acs.jctc.4c01512](https://doi.org/10.1021/acs.jctc.4c01512).

(14) Bomble, Y. J.; Stanton, J. F.; Kállay, M.; Gauss, J. Coupled-cluster methods including noniterative corrections for quadruple excitations. *J. Chem. Phys.* **2005**, *123*, 054101, DOI: [10.1063/1.1950567](https://doi.org/10.1063/1.1950567).

(15) Lambie, S.; Kats, D.; Usvyat, D.; Alavi, A. On the applicability of CCSD(T) for dispersion interactions in large conjugated systems. *J. Chem. Phys.* **2025**, *162*, 114112, DOI: 10.1063/5.0246763.

(16) Hobza, P.; Selzle, H. L.; Schlag, E. W. Potential Energy Surface for the Benzene Dimer. Results of ab Initio CCSD(T) Calculations Show Two Nearly Isoenergetic Structures: T-Shaped and Parallel-Displaced. *J. Phys. Chem.* **1996**, *100*, 18790–18794, DOI: 10.1021/jp961239y.

(17) Hohenberg, P.; Kohn, W. Inhomogeneous Electron Gas. *Phys. Rev.* **1964**, *136*, B864–B871, DOI: 10.1103/PhysRev.136.B864.

(18) Kohn, W.; Sham, L. J. Self-Consistent Equations Including Exchange and Correlation Effects. *Phys. Rev.* **1965**, *140*, A1133–A1138, DOI: 10.1103/PhysRev.140.A1133.

(19) Mardirossian, N.; Head-Gordon, M. Mapping the Genome of Meta-Generalized Gradient Approximation Density Functionals: The Search for B97M-V. *J. Chem. Phys.* **2015**, *142*, 074111, DOI: 10.1063/1.4907719.

(20) Weigend, F.; Ahlrichs, R. Balanced basis sets of split valence, triple zeta valence and quadruple zeta valence quality for H to Rn: Design and assessment of accuracy. *Phys. Chem. Chem. Phys.* **2005**, *7*, 3297–3305, DOI: 10.1039/B508541A.

(21) Neese, F.; Wennmohs, F.; Becker, U.; Ripplinger, C. The ORCA quantum chemistry program package. *J. Chem. Phys.* **2020**, *152*, 224108, DOI: 10.1063/5.0004608.

(22) Epifanovsky, E.; Zuev, D.; Feng, X.; Khistyayev, K.; Shao, Y.; Krylov, A. I. General implementation of the resolution-of-the-identity and Cholesky representations of electron repulsion integrals within coupled-cluster and equation-of-motion methods: Theory and benchmarks. *J. Chem. Phys.* **2013**, *139*, 134105, DOI: 10.1063/1.4820484.

(23) Shen, T.; Zhu, Z.; Zhang, I. Y.; Scheffler, M. Massive-parallel implementation of the resolution-of-identity coupled-cluster approaches in the numeric atom-centered orbital framework for molecular systems. *J. Chem. Theory Comput.* **2019**, *15*, 4721–4734, DOI: 10.1021/acs.jctc.8b01294.

(24) Kállay, M.; Nagy, P. R.; Mester, D.; Rolik, Z.; Samu, G.; Csontos, J.; Csóka, J.; Szabó, P. B.; Gyevi-Nagy, L.; Hégely, B. et al. The MRCC program system: Accurate quantum chemistry from water to proteins. *J. Chem. Phys.* **2020**, *152*, 074107, DOI: 10.1063/1.5142048.

(25) Nagy, P. R.; Kállay, M. Approaching the Basis Set Limit of CCSD(T) Energies for Large Molecules with Local Natural Orbital Coupled-Cluster Methods. *J. Chem. Theory Comput.* **2019**, *15*, 5275–5298, DOI: 10.1021/acs.jctc.9b00538.

(26) Nagy, P. R. State-of-the-art local correlation methods enable accurate and affordable gold standard quantum chemistry up to a few hundred atoms. *Chem. Sci.* **2024**, *15*, 14556, DOI: 10.1039/D4SC04755A.

(27) Ripplinger, C.; Neese, F. An efficient and near linear scaling pair natural orbital based local coupled cluster method. *J. Chem. Phys.* **2013**, *138*, 034106, DOI: 10.1063/1.4773581.

(28) Ripplinger, C.; Sandhoefer, B.; Hansen, A.; Neese, F. Natural triple excitations in local coupled cluster calculations with pair natural orbitals. *J. Chem. Phys.* **2013**, *139*, 134101, DOI: 10.1063/1.4821834.

(29) Ma, Q.; Werner, H.-J. Explicitly correlated local coupled-cluster methods using pair natural orbitals. *Wiley Interdisciplinary Reviews: Computational Molecular Science* **2018**, *8*, e1371, DOI: 10.1002/wcms.1371.

(30) Werner, H.-J.; Knowles, P. J.; Knizia, G.; Manby, F. R.; Schütz, M. MOLPRO: a general-purpose quantum chemistry program package. *WIREs Computational Molecular Science* **2020**, *10*, e1427, DOI: 10.1002/wcms.1427.

(31) Stanton, J. F.; Gauss, J. A simple correction to final state energies of doublet radicals described by equation-of-motion coupled cluster theory in the singles and doubles approximation. *Theor. Chem. Acc.* **1996**, *93*, 303–313, DOI: [10.1007/s002140050154](https://doi.org/10.1007/s002140050154).

(32) Crawford, T. D.; Stanton, J. F. Investigation of an asymmetric triple-excitation correction for coupled-cluster energies. *Int. J. Quantum Chem.* **1998**, *70*, 601–611, DOI: [10.1002/\(sici\)1097-461x\(1998\)70:4/5<601::aid-qua6>3.0.co;2-z](https://doi.org/10.1002/(sici)1097-461x(1998)70:4/5<601::aid-qua6>3.0.co;2-z).

(33) Kucharski, S. A.; Bartlett, R. J. Noniterative energy corrections through fifth-order to the coupled cluster singles and doubles method. *J. Chem. Phys.* **1998**, *108*, 5243–5254, DOI: [10.1063/1.475961](https://doi.org/10.1063/1.475961).

(34) Kucharski, S. A.; Bartlett, R. J. Sixth-order energy corrections with converged coupled cluster singles and doubles amplitudes. *J. Chem. Phys.* **1998**, *108*, 5255–5264, DOI: [10.1063/1.475962](https://doi.org/10.1063/1.475962).

(35) Matthews, D. A.; Cheng, L.; Harding, M. E.; Lipparini, F.; Stopkowicz, S.; Jagau, T.-C.; Szalay, P. G.; Gauss, J.; Stanton, J. F. Coupled-cluster techniques for computational chemistry: The CFOUR program package. *J. Chem. Phys.* **2020**, *152*, 214108, DOI: [10.1063/5.0004837](https://doi.org/10.1063/5.0004837).

(36) Stanton, J. F. Why CCSD(T) works: a different perspective. *Chem. Phys. Lett.* **1997**, *281*, 130–134, DOI: [10.1016/S0009-2614\(97\)01144-5](https://doi.org/10.1016/S0009-2614(97)01144-5).

(37) Noga, J.; Bartlett, R. J.; Urban, M. Towards a full CCSDT model for electron correlation. CCSDT-n models. *Chem. Phys. Lett.* **1987**, *134*, 126–132, DOI: [10.1016/0009-2614\(87\)87107-5](https://doi.org/10.1016/0009-2614(87)87107-5).

(38) Møller, C.; Plesset, M. S. Note on an approximation treatment for many-electron systems. *Phys. Rev.* **1934**, *46*, 618, DOI: [10.1103/PhysRev.46.618](https://doi.org/10.1103/PhysRev.46.618).

(39) Loipersberger, M.; Bertels, L. W.; Lee, J.; Head-Gordon, M. Exploring the Limits of Second- and Third-Order Møller–Plesset Perturbation Theories for Noncovalent Interactions: Revisiting MP2.5 and Assessing the Importance of Regularization and Reference Orbitals. *J. Chem. Theory Comput.* **2021**, *17*, 5582–5599, DOI: 10.1021/acs.jctc.1c00469.

(40) Shao, Y.; Gan, Z.; Epifanovsky, E.; Gilbert, A. M.; Wormit, M.; Kussmann, J.; Lange, A. W.; He, X.; Diedenhofen, T. G. W.; Walker, M. A. et al. Advances in Molecular Quantum Chemistry Contained in the Q-Chem 4 Program Package. *Mol. Phys.* **2015**, *113*, 184–215, DOI: 10.1080/00268976.2014.952696.

(41) Dunning Jr, T. H. Gaussian basis sets for use in correlated molecular calculations. I. The atoms boron through neon and hydrogen. *J. Chem. Phys.* **1989**, *90*, 1007–1023, DOI: 10.1063/1.456153.

(42) Woon, D. E.; Dunning Jr, T. H. Gaussian basis sets for use in correlated molecular calculations. III. The atoms aluminum through argon. *J. Chem. Phys.* **1993**, *98*, 1358–1371, DOI: 10.1063/1.464303.

(43) Martin, J. M. L.; Santra, G.; Semidalas, E. An exchange-based diagnostic for static correlation. *AIP Conf. Proc.* **2022**, *2611*, 020014, DOI: 10.1063/5.0119280.

(44) Řezáč, J.; Riley, K. E.; Hobza, P. S66: A Well-balanced Database of Benchmark Interaction Energies Relevant to Biomolecular Structures. *J. Chem. Theory Comput.* **2011**, *7*, 2427–2438, DOI: 10.1021/ct2002946.

(45) Masumian, E.; Boese, A. D. Benchmarking Swaths of Intermolecular Interaction Components with Symmetry-Adapted Perturbation Theory. *J. Chem. Theory Comput.* **2023**, *20*, 30–48, DOI: 10.1021/acs.jctc.3c00801.

(46) Semidalas, E.; Boese, A. D.; Martin, J. M. Post-CCSD (T) corrections in the S66

noncovalent interactions benchmark. *Chem. Phys. Lett.* **2025**, *863*, 141874, DOI: 10.1016/j.cplett.2025.141874.

(47) Schäfer, T.; Irmler, A.; Gallo, A.; Grüneis, A. Understanding discrepancies in noncovalent interaction energies from wavefunction theories for large molecules. *Nat. Commun.* **2025**, *16*, 9108, DOI: 10.1038/s41467-025-64104-8.

(48) Villot, C.; Ballesteros, F.; Wang, D.; Lao, K. U. Coupled cluster benchmarking of large noncovalent complexes in L7 and S12L as well as the C60 dimer, DNA-ellipticine, and HIV-indinavir. *J. Phys. Chem. A* **2022**, *126*, 4326–4341, DOI: 10.1021/acs.jpca.2c01421.

(49) Hansen, A.; Knowles, P. J.; Werner, H.-J. Accurate calculation of noncovalent interactions using PNO-LCCSD(T)-F12 in Molpro. *J. Phys. Chem. A* **2025**, *129*, 4812–4833, DOI: 10.1021/acs.jpca.5c02316.

(50) Lao, K. U. Canonical coupled cluster binding benchmark for nanoscale noncovalent complexes at the hundred-atom scale. *J. Chem. Phys.* **2024**, *161*, 234103, DOI: 10.1063/5.0242359.

(51) Benali, A.; Shin, H.; Heinonen, O. Quantum Monte Carlo benchmarking of large noncovalent complexes in the L7 benchmark set. *J. Chem. Phys.* **2020**, *153*, 194113, DOI: 10.1063/5.0026275.

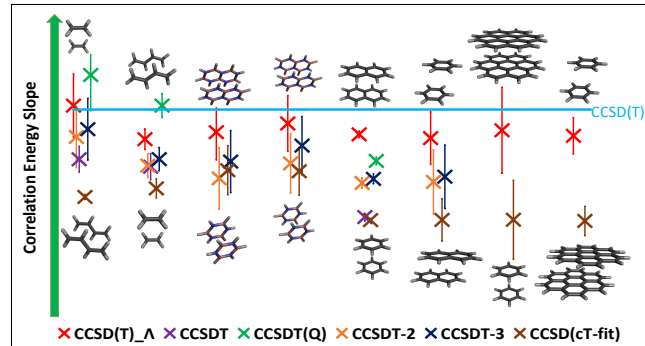
(52) Shi, B. X.; Della Pia, F.; Al-Hamdani, Y. S.; Michaelides, A.; Alfè, D.; Zen, A. Systematic discrepancies between reference methods for noncovalent interactions within the S66 dataset. *J. Chem. Phys.* **2025**, *162*, 144107, DOI: 10.1063/5.0254021, Published online 2025-04-09.

(53) Awasthi, D.; Otis, L.; Huang, E.; Shee, J. Noncovalent Interaction Energies with Phaseless Auxiliary-Field Quantum Monte Carlo. *J. Chem. Theory Comput.* **2026**, *22*, 264–275, DOI: 10.1021/acs.jctc.5c01477, Published online 2025-12-16.

(54) Fanta, R.; Jurečka, P.; Dubecký, M. Why Nondynamic Correlation Matters for  $\pi\pi$  Stacking? Lessons from the Benzene Dimer. *J. Phys. Chem. Lett.* **2025**, *16*, 10982–10988, DOI: 10.1021/acs.jpclett.5c02576.

(55) Lambie, S.; López-Ríos, P.; Kats, D.; Alavi, A. Nodal error behind discrepancies between coupled cluster and diffusion Monte Carlo: AcOH dimer case study. 2025; <https://arxiv.org/abs/2508.17937>, arXiv:2508.17937 [physics.chem-ph], submitted 2025-08-25.

# TOC Graphic



By considering the evolution of the correlation binding energy with respect to the number of subunits of dimer interactions, deviations from the reference CCSD(T) method scale linearly to ever larger systems. Overall, eight linear series are investigated.